Complex conductivity of polyacetylene films prepared by different methods

Kohzo Ito*,† and Yoshikazu Tanabe
Research Institute for Polymers and Textiles, Tsukuba, Ibaraki 305, Japan

Kazuo Akagi and Hideki Shirakawa
Institute of Materials Science, University of Tsukuba, Tsukuba, Ibaraki 305, Japan
(Received 17 June 1991)

The frequency (f) and temperature (T) dependence of the complex conductivity σ^* was measured for undoped and lightly doped films of highly stretchable polyacetylene (hs-PA) and Shirakawa polyacetylene (S-PA). When σ^* and f were reduced by using the dc conductivity $\sigma(0)$, all the experimental data of σ^* of hs-PA were on a master curve whereas those of S-PA did not show such universality. The data analysis based on the conductivity relaxation formalism revealed that the functional form $H(\tau) \propto \tau^{\alpha}$ ($\tau_{\min} < \tau < \tau_{\max}$, $-1 < \alpha < 1$) of the relaxation spectrum $H(\tau)$, i.e., the distribution function of relaxation time τ, fitted the experimental data best and that α was independent of T for hs-PA while α was proportional to T for S-PA. The T-independent α for hs-PA indicates isoenergetic hopping between equivalent sites, so that the conduction mechanism in hs-PA can be ascribed to acoustic-phonon-assisted hopping of charged solitons between PA chains. On the other hand, it is likely that the inter-fibril-barrier hopping makes the main contribution to the conduction mechanism in S-PA. This difference in conduction mechanisms between hs-PA and S-PA is attributed to their morphological dissimilarities.

I. INTRODUCTION

Conducting polymers have been extensively investigated by physicists and chemists since polyacetylene (PA) was found to show a notable increase in dc conductivity $\sigma(0)$ with increasing dopant concentration in 1977.[1,2] As a result, many different conducting polymers have been developed to achieve higher dc conductivities. Besides producing conducting films with high conductivity and practical stability, an understanding of the conduction mechanism in conducting polymers is also one of the main goals of these investigations. However, few detailed pictures of the conduction mechanism have been obtained even for PA, although various models were proposed.[2] The impedance spectroscopy[3] (or complex conductivity measurement) is an effective technique to reveal the conduction mechanism in conducting polymers, in particular undoped and lightly doped ones. For instance, the complex conductivity σ^* (or ac conductivity) yields information on the distribution of intramolecular and intermolecular hopping rates, which should be widely distributed in disordered or semiordered materials such as conducting polymers. One can then obtain the temperature dependence of the hopping rate from that of the distribution by measuring σ^* at various temperatures. On the other hand, it would be difficult from a measurement of the dc conductivity $\sigma(0)$ alone to acquire information on individual hopping rates since $\sigma(0)$ reflects the summation of all the hopping rates in the distribution. As a consequence, σ^* measurements over wide frequency and temperature ranges are expected to lead us to a more detailed understanding of the conduction mechanism in conducting polymers.

It is widely believed that solitons play an important role in conduction in PA films.[2,4] Particularly in undoped and lightly doped PA, a charged soliton is thought to make the main contribution to the conductivity as a carrier. Epstein *et al.*[5] measured σ^* of an undoped PA film (S-PA) synthesized by the Shirakawa method,[6] and indicated that the experimental results could be explained by the intersoliton hopping (ISH) model.[7] In the ISH model the main contribution to the conductivity comes from the intermolecular hopping of the charge between a charged soliton bound to a dopant and a neutral soliton near another dopant. On the other hand, Chroboczek and Summerfield[8] reported that their experimental results of σ^* for undoped S-PA films did not agree with the ISH model but could be interpreted in terms of the extended pair approximation (EPA) with the energy-dependent hopping model. It is, however, still controversial as to which of the conduction mechanisms, among others, properly explains the experimental results of undoped S-PA. This is partly because one does not have enough experimental results to determine the conduction mechanism.

PA synthesized with aged catalyst at high temperature has recently attracted interest of the researchers on conducting polymers owing to its high conductivity and stability.[9,10] Akagi *et al.*[11] reported that highly stretchable polyacetylene (hs-PA), which is polymerized by the nonsolvent method with aged catalyst at high temperature, showed much higher dc conductivity, bulk density, and Young's modulus than those in S-PA. The difference in stretchability between hs-PA and S-PA is closely related to dissimilarities in morphology or the higher-order structure.[11,12] For instance, a fibrillar structure[2] is observed in S-PA while a densely packed granular structure is found in hs-PA.[12] This morphological difference between hs-PA and S-PA is expected to affect their conduction mechanisms.

The purpose of this study is to reveal the conduction mechanism of undoped and lightly doped PA by measuring the frequency (f) and temperature (T) dependence of σ^* for undoped and lightly doped hs-PA and S-PA films. As mentioned earlier, σ^* reflects the distribution of hopping rates and yields information on separate hopping rates, of which the T dependence characterizes the conduction mechanism. Thus, we will discuss which mechanism best fits the respective experimental results of hs-PA and S-PA in this study. It is expected that a comparison of σ^* between hs-PA and S-PA may elucidate the effect of the higher-order structure on the conduction mechanism in PA.

II. EXPERIMENT

Preparation conditions of hs-PA and S-PA samples used in this study are summarized in Table I. The hs-PA films with thicknesses of approximately 25 μm were synthesized at $-78\,^{\circ}C$ by using the catalyst $[Ti(OBu)_4/AlEt_3]$ aged at 150 °C for five hours with the refined nonsolvent method.[11] The S-PA films with thicknesses of approximately 150 μm were prepared by the Shirakawa method.[6]

Iodine doping was performed in carbon tetrachloride solutions with various concentrations of iodine after the as-prepared *cis*-rich PA films were annealed at approximately 170 °C for 30 min under vacuum to convert them into the *trans* isomers. The complete isomerization was confirmed by using differential scanning calorimetry. The concentration (y) of iodine $[CHI_y]_n$ in doped films was determined by the weight uptake.

The σ^* measurement was carried out by using an arbitrary waveform generator (Wavetek Model No. 75) and a fast Fourier transform analyzer (Advantest TR9407) in the frequency (50 mHz to 1 MHz) and temperature (-90 K to room temperature) ranges. The multifrequency simultaneous method[13] was employed to avoid the effect of the temperature drift on σ^* during the measurements. The electrodes used were of the parallel condenser type, that is, a PA film was sandwiched between two gold electrodes vacuum deposited. A strongly non-Ohmic behavior was observed in the lightly doped hs-PA samples. Thus, we applied small enough amplitude of voltage to the samples to avoid the non-Ohmic effect on the σ^* measurement.

III. RESULTS AND DATA ANALYSIS

As a typical example, Fig. 1 shows the f and T dependence of (a) $\mathrm{Re}(\sigma^*)$ and (b) $\mathrm{Re}(\epsilon^*)$ for the lightly doped hs-PA samples ($y = 5.0\times10^{-4}$), where ϵ^* is the complex dielectric constant which is defined by

$$\sigma^* = i\omega\epsilon_0\epsilon^* \,. \tag{1}$$

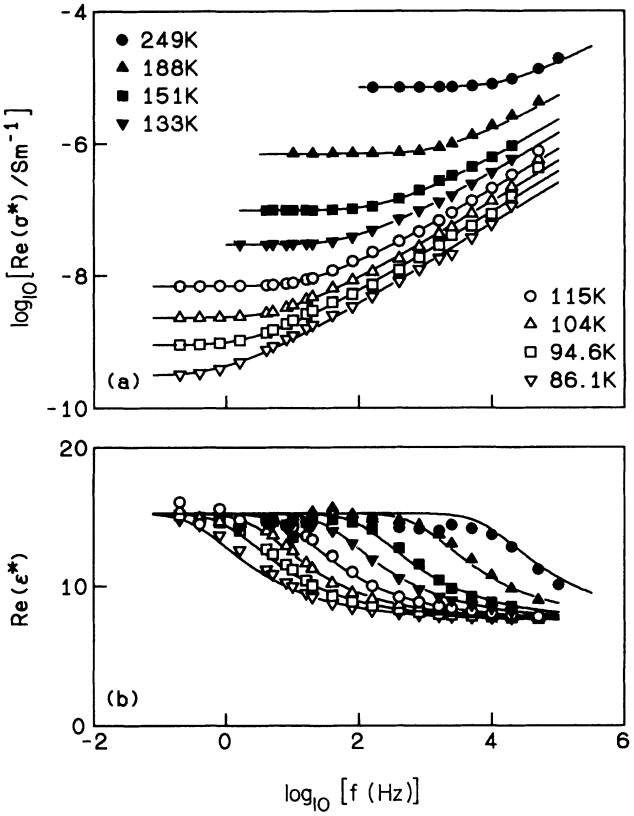

FIG. 1. The f dependence of (a) $\mathrm{Re}(\sigma^*)$ and (b) $\mathrm{Re}(\epsilon^*)$ at different temperatures for the lightly doped hs-PA sample ($y = 5.0\times10^{-4}$). The solid curves were obtained from Eq. (3) with Eq. (4).

Here ω is the angular frequency and ϵ_0 the vacuum permittivity. As shown in Fig. 1, $\mathrm{Re}(\sigma^*)$ is proportional to f^s with the slope s in the frequency range higher than the relaxation frequency f_r which is roughly estimated from the inflection frequency in $\mathrm{Re}(\sigma^*)$ or $\mathrm{Re}(\epsilon^*)$. Also, both the dc conductivity $\sigma(0)$ and f_r depend strongly on T whereas the dielectric increment $\Delta\epsilon$, defined by the difference between the low-frequency $[\epsilon(0)]$ and the high-frequency $[\epsilon(\infty)]$ limits of $\mathrm{Re}(\epsilon^*)$, is almost independent of T. The plot of $\sigma(0)$ versus T^{-1} for this sample is exhibited by the symbol $\triangle$ in Fig. 2, together with other undoped and lightly doped hs-PA samples. Figure 2 shows that $\sigma(0)$ of hs-PA has the non-Arrhenius type of T dependence. In Fig. 3, we replotted all the experimental data in Fig. 1 by using reduced parameters $\sigma^*/\sigma(0)$ and $f\epsilon_0/\sigma(0)$ which correspond to σ^* and f, respectively. Here, the relation among σ^*, ϵ^*, and f in Eq. (1) is replaced with that among the reduced parameters $\sigma^*/\sigma(0)$, ϵ^* and $f\epsilon_0/\sigma(0)$ as

TABLE I. Preparation conditions of the hs-PA and S-PA samples used in this study.

Sample	Solvent	Aging T (°C)	Polymerization T (°C)	Time	Max. draw Ratio	*cis* content (%)
hs-PA	nonsolvent	150–160	−78	20 h	8	93
S-PA	toluene	RT	−78	6 min	3	95

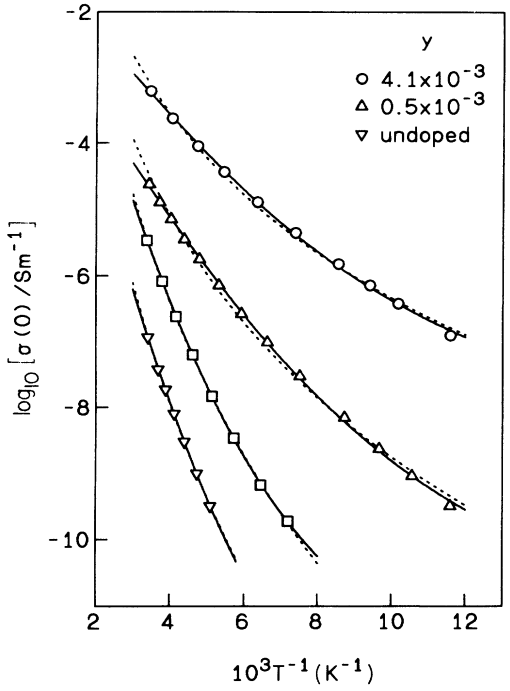

FIG. 2. Plot of $\sigma(0)$ vs T^{-1} for the hs-PA samples where the symbol □ denotes the slightly doped sample with the dc conductivity of 3.42×10^{-6} Sm^{-1} at room temperature. The solid curves were obtained from Eq. (5) and the dashed ones from the ISH model

$$\sigma^*/\sigma(0)=i[\omega\epsilon_0/\sigma(0)]\epsilon^* \ . \tag{2}$$

Figure 3 shows that all the experimental data are on a master curve, which indicates that the slope s of f^s is independent of T and that f_r has the same T dependence as $\sigma(0)$. This means that the T dependence of σ^* is ascribed to that of $\sigma(0)$ completely. This universality of σ^* with respect to the parameters reduced by $\sigma(0)$ manifested itself in all the undoped and lightly doped hs-PA samples measured.

In contrast, the *S*-PA samples did not show such universality concerning the reduced parameters $\sigma^*/\sigma(0)$ and $f\epsilon_0/\sigma(0)$, although the close relation between $\sigma(0)$ and f_r was observed as seen in the hs-PA samples. A typical example of the *S*-PA samples is shown in Fig. 4 ($y=4.8\times10^{-4}$) where the slope s and the dielectric increment $\Delta\epsilon$ decrease with increasing T. Figure 5 shows the plot of $\sigma(0)$ versus T^{-1} for the undoped and lightly doped *S*-PA samples including the above one in the symbol △. Similar to the hs-PA samples, $\sigma(0)$ showed the non-Arrhenius type of T dependence. In Fig. 6, we replotted the experimental data in Fig. 4 by using the reduced parameters $\sigma^*/\sigma(0)$ and $f\epsilon_0/\sigma(0)$ but did not obtain a master curve. This indicates that the T dependence of σ^* does not result form that of only $\sigma(0)$ but also from both s and $\Delta\epsilon$ decreasing with increasing T. This T-dependent s and $\Delta\epsilon$ were observed in all the un-

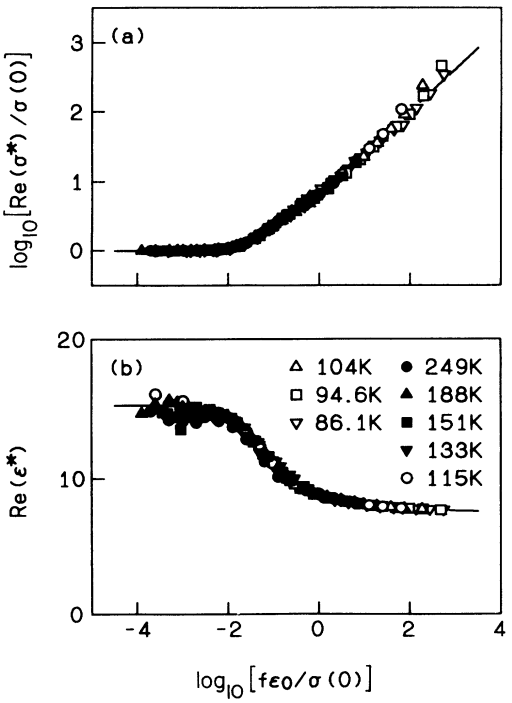

FIG. 3. The dependence of (a) $\mathrm{Re}[\sigma^*/\sigma(0)]$ and (b) $\mathrm{Re}(\epsilon^*)$ on the reduced frequency $f\epsilon_0/\sigma(0)$ for the lightly doped hs-PA sample ($y=5.0\times10^{-4}$). The solid curves were obtained from Eq. (3) with Eq. (4).

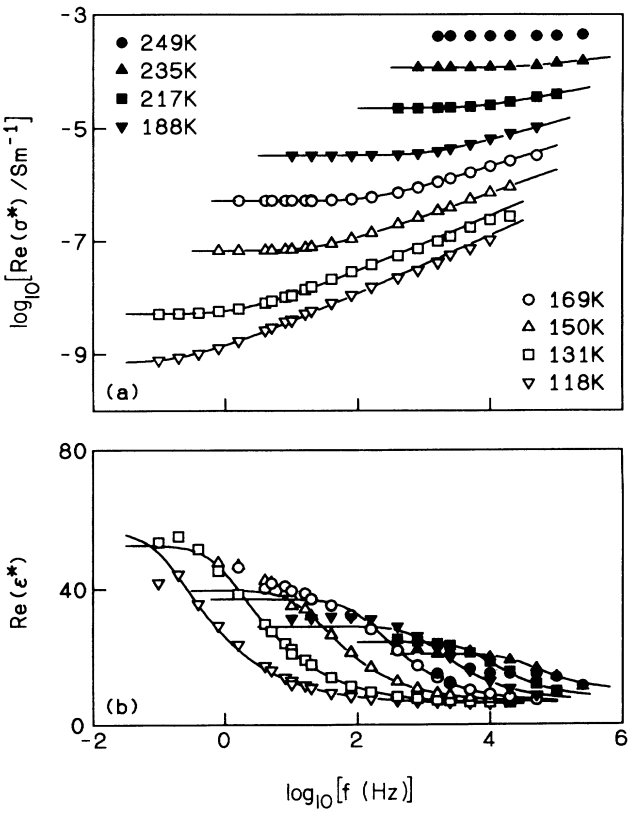

FIG. 4. The f dependence of (a) $\mathrm{Re}(\sigma^*)$ and (b) $\mathrm{Re}(\epsilon^*)$ at different temperatures for the lightly doped *S*-PA sample ($y=4.8\times10^{-4}$). The solid curves were obtained from Eq. (3) with Eq. (4).

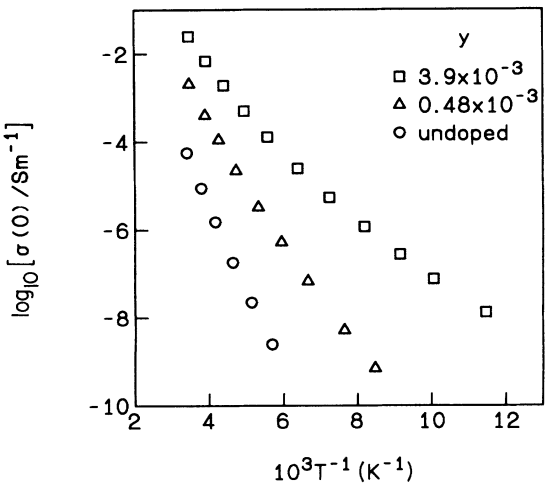

FIG. 5. Plot of $\sigma(0)$ vs T^{-1} for the S-PA samples.

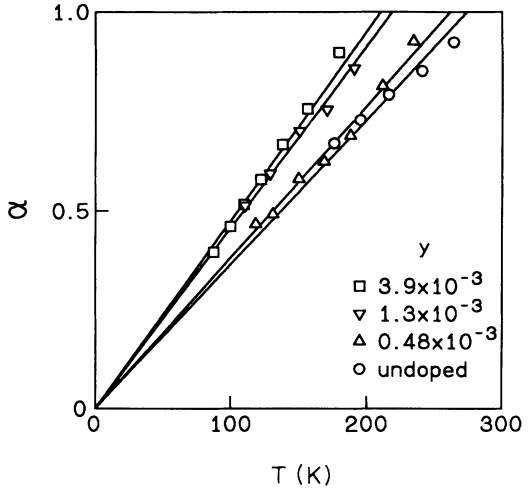

FIG. 7. The T dependence of α for all the S-PA samples.

doped and lightly doped S-PA samples.

A difference between hs-PA and S-PA was also observed in the non-Ohmic behavior.[14] The lightly doped hs-PA samples showed strongly non-Ohmic behavior, of which the nonlinearity increased gradually with decreasing T. In contrast, such a strongly non-Ohmic behavior did not manifest itself in the S-PA samples.

In general, the f dependence in disordered materials that $\mathrm{Re}(\sigma^*)$ increases monotonically with increasing f arises from the dielectric relaxation due to the local mechanism such as the dipole moment rotation and the charge polarization or from the conductivity relaxation caused by the long-range transport mechanism of a carrier hopping with multiple relaxation times τ.[15] The dielectric relaxation makes no contributions to $\sigma(0)$ while the conductivity relaxation yields $\sigma(0)$ in the low-frequency limit. The present experimental result of the close relation between $\sigma(0)$ and f_r in the T dependence indicates that they result from the same conduction mechanism, so that both the f dependences of hs-PA and S-PA should be ascribed to the conductivity relaxation. In this case, one ought not to employ the widely adopted analysis scheme of the experimental data in which $\sigma(0)$ and σ_{ac}, defined by $\sigma_{ac}=\mathrm{Re}(\sigma^*)-\sigma(0)$, are dealt with and discussed separately, but to adopt the analysis scheme based on the conductivity relaxation formalism where $\sigma(0)$ is regarded as the low-frequency limit of $\mathrm{Re}(\sigma^*)$.[15]

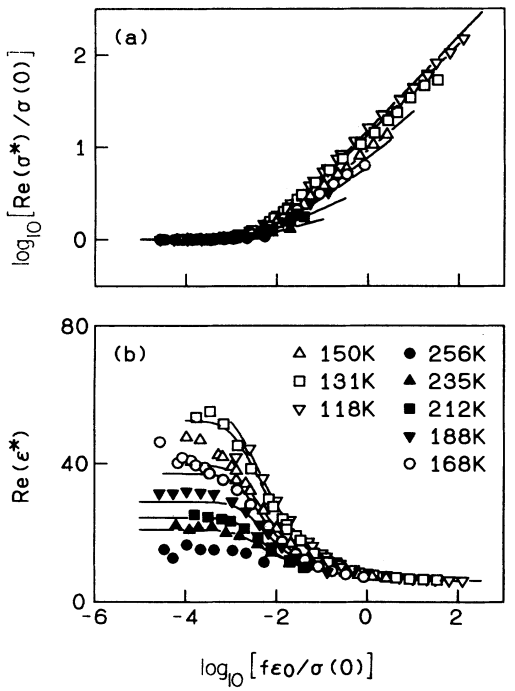

FIG. 6. The dependence of (a) $\mathrm{Re}[\sigma^*/\sigma(0)]$ and (b) $\mathrm{Re}(\epsilon^*)$ on the reduced frequency $f\epsilon_0/\sigma(0)$ for the lightly doped S-PA sample ($y=4.8\times10^{-4}$). The solid curves were obtained from Eq. (3) with Eq. (4).

The conductivity relaxation, i.e., the long-range hopping of a carrier, has been treated by several theoretical studies,[16] which led to the relation between σ^* and the distribution of relaxation time τ, i.e., the normalized relaxation spectrum $H(\tau)$. Here, we will adopt the relation derived from the continuous time random walk,[17,18]

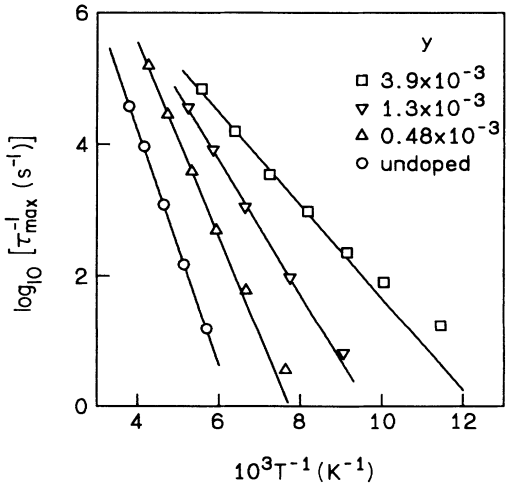

FIG. 8. Plot of τ_{max}^{-1} vs T^{-1} for the S-PA samples.

TABLE II. The best-fitting values of K and $\tau_{max}\sigma(0)/\epsilon_0$ for the positive and negative α in all the hs-PA samples by using Eq. (3) with Eq. (4). Here blank spaces indicate that the weight uptake is too small to be determined.

$y\times10^{-3}$	$\sigma(0)$ (Sm^{-1}) at RT	K_+	α_+	$\tau_{max+}\sigma(0)/\epsilon_0$	K_-	α_-	$\tau_{max-}\sigma(0)/\epsilon_0$
undoped	1.16×10^{-7}	18.4	0.56	48.7	1.93×10^{-3}	−0.59	40.6
	5.07×10^{-7}	3.01	0.50	8.66	2.16×10^{-3}	−0.52	6.70
	3.42×10^{-6}	7.99	0.46	24.9	4.76×10^{-3}	−0.50	19.3
	9.78×10^{-6}	2.94	0.35	10.9	1.11×10^{-2}	−0.40	9.54
0.5	2.38×10^{-5}	6.76	0.34	26.8	2.34×10^{-2}	−0.37	20.1
1.3	7.63×10^{-5}	7.39	0.25	37.1	2.06×10^{-2}	−0.40	30.8
3.0	4.98×10^{-4}	2.16	0.78	4.82	9.03×10^{-5}	−0.80	7.19
4.1	6.10×10^{-4}	9.71	0.83	21.3	2.61×10^{-4}	−0.73	19.0

$$\sigma^*=K\epsilon_0\left\{-i\omega+\left[\int_{\tau_{min}}^{\tau_{max}}H(\tau)(1+i\omega\tau)^{-1}d\tau\right]^{-1}\right\}+i\omega\epsilon_0\epsilon(\infty)\ , \tag{3}$$

for the analysis of the experimental data. In Eq. (3), K is a constant proportional to the number density of carriers. By assuming the specific functional form of $H(\tau)$ and fitting Eq. (3) to the experimental data of σ^*, we found the form

$$H(\tau)\propto\tau^{\alpha}\quad(\tau_{min}<\tau<\tau_{max},\quad -1<\alpha<1) \tag{4}$$

best fitting in most cases as shown typically in the solid curves in Figs. 1, 3, 4, and 6. The experimental result of the hs-PA samples that all the data were on a master curve indicates that the parameter α, characterizing the sharpness in the profile for $H(\tau)$, is independent of T. [Equation (3) combined with Eq. (4) yields the f dependence of $\mathrm{Re}(\sigma^*)\propto f^{1-|\alpha|}$ in $\tau_{max}^{-1}\ll\omega\ll\tau_{min}^{-1}$. Thus, the T-independent α corresponds to a constant slope $s=1-|\alpha|$ of f^s.] Fitting Eq. (3) with Eq. (4) to the experimental data, we obtained two sets of the best-fitting parameters for positive and negative values of α. Table II summarizes the result of all the hs-PA samples, where K_+ and τ_{max+} correspond to the positive α_+ while K_- and τ_{max-} correspond to the negative α_-. Since the frequency range in this study should be much lower than τ_{min}^{-1}, we can assume τ_{min} arbitrarily with no influence on the values of the best-fitting parameters except K_-. Thus, we adopted $\tau_{min}=10^{-6}\epsilon_0/\sigma(0)$ in this data analysis to obtain the best-fitting parameters. Table II indicates that the average value α of α_+ and $|\alpha_-|$, which are almost the same, increases gradually with y in the lightly doped hs-PA samples ($y\geq5.0\times0^{-4}$). Incidentally, the master curve in Fig. 3 suggests that $\tau_{max}^{-1}\sim2\pi f_r$ has the same T dependence as $\sigma(0)$ shown in Fig. 2, and hence that $\tau_{max}\sigma(0)/\epsilon_0$ in Table II is independent of T.

Whereas the parameter α or the profile for $H(\tau)$ was independent of T in hs-PA, the S-PA sample showed the T-dependent α. Thus, we fitted Eq. (3) with Eq. (4) to the experimental data of the lightly doped S-PA sample at different temperatures as indicated by the solid curves in Figs. 4 and 6. The best-fitting parameters are summarized in Table III, where α_+ and $|\alpha_-|$ are almost the same. The average value α of α_+ and $|\alpha_-|$ in Table III was plotted versus T in the symbol △ in Fig. 7, together with the other undoped and lightly doped S-PA samples measured. Figure 7 shows that α of the S-PA samples is proportional to T, which means that the profile for $H(\tau)$ increases its sharpness as T rises. This T-dependent profile for $H(\tau)$ in S-PA ought to affect the T dependence of $\sigma(0)$ as suggested in Eq. (3), which results in the different T dependence between $\sigma(0)$ and τ_{max}^{-1} in S-PA. For comparison, the plot of the average value τ_{max}^{-1} of τ_{max+}^{-1} and τ_{max-}^{-1} versus T^{-1} is shown in Fig. 8.

IV. DISCUSSION

As mentioned in Sec. I, two groups have reported the experimental results of σ^* for the undoped S-PA sample, leading to the different conclusions, the ISH model and the EPA, on the conduction mechanism of PA. In the ISH model, all the hopping sites are assumed to be equivalent regarding the energy level, which is called the isoenergetic hopping.[19] This means that $H(\tau)$ results from the distribution of the hopping distance only,[7] so

TABLE III. The best-fitting values of K and $\tau_{max}\sigma(0)/\epsilon_0$ for the positive and negative α at different temperatures in the S-PA sample ($y=4.8\times10^{-4}$) by using Eq. (3) with Eq. (4).

T (K)	K_+	α_+	$\tau_{max+}\sigma(0)/\epsilon_0$	K_-	α_-	$\tau_{max-}\sigma(0)/\epsilon_0$
235	34.4	0.97	69.9	5.75×10^{-5}	−0.88	92.6
217	40.4	0.85	87.7	1.93×10^{-4}	−0.78	91.8
188	43.8	0.71	104	9.13×10^{-4}	−0.67	88.9
169	49.4	0.63	128	1.76×10^{-3}	−0.62	112
150	52.8	0.58	142	3.36×10^{-3}	−0.58	111
131	60.4	0.48	186	1.13×10^{-2}	−0.50	139
118	57.1	0.45	175	1.61×10^{-2}	−0.48	142

that the profile for $H(\tau)$ is independent of T. Thus, the conduction mechanism of hs-PA should be ascribed to the isoenergetic hopping. On the other hand, the energy-dependent hopping model such as the EPA can give us the T-dependent profile for $H(\tau)$. In the following subsections we will individually consider the conduction mechanism of hs-PA and S-PA in detail.

A. hs-PA

First of all, we will discuss whether the experimental data of hs-PA agree with the ISH model or not. This theory is characterized by the hopping rate $\Gamma=\tau^{-1}$ proportional to T^n ($n\simeq 10$).[7] The dashed curves in Fig. 2 are the theoretical ones which were obtained by the least-squares method with the functional form $\sigma(0)\propto\Gamma\propto T^n$. Figure 2 indicates that the theoretical curves deviate appreciably from the experimental data throughout the temperature regime for the measurement. Although this deviation becomes obscure in the undoped and slightly doped hs-PA samples, of which the experimental data were obtained only in the narrow temperature regime, it ought to be concluded that the ISH model cannot explain the experimental data of the T dependence of hs-PA.

Whereas the characteristic T dependence of τ^{-1} in the ISH model was derived from the interaction between the soliton and the phonon in PA chains,[7] a more detailed theory of a phonon-assisted hopping has been dealt with by Emin.[20–22] For the optical phonon with the frequency ω_0, the isoenergetic hopping rate $\Gamma(0)=\tau^{-1}$ for jumps between equivalent sites was given in the limit of weak vibrational dispersion as[21]

$$\Gamma(0)=(J/\hbar)^2(2\pi/\omega_0)\exp[-(2E_b/\hbar\omega_0)\coth(\hbar\omega_0/2kT)]\times\{I_0[(2E_b/\hbar\omega_0)\operatorname{csch}(\hbar\omega_0/2kT)]-1\}\ , \quad (5)$$

where I_0 represents the zeroth-order modified Bessel function, J is the transfer integral, E_b the binding energy, and kT the thermal energy. It was indicated that Eq. (5) was reduced to the Arrhenius type of T dependence in each of the high- and low-temperature limits: the activation energies are given by $E_b/2$ in the high-temperature regime ($\hbar\omega_0/kT<3$) and by $\hbar\omega_0$ in the low-temperature regime ($\hbar\omega_0/kT>3$).[21] On the other hand, the same asymptotic expression of the isoenergetic hopping rate as that derived from Eq. (5), i.e., the activated T dependence with the activation energy $E_b/2$, was obtained for the acoustic phonon in the high-temperature regime ($\hbar\omega_m/kT<3$).[22] Here ω_m, defined by $\omega_m=\omega_D/l$, denotes the angular frequency of the highest-energy vibration mode with which the carrier can effectively interact, where ω_D is the Debye frequency and l is the ratio of the radii of the carrier to the average lattice spacing.[20,23] In the lower-temperature regime ($\hbar\omega_m/kT>3$), the large dispersion of the acoustic phonon gives rise to a nonactivated T dependence of the hopping rate in contrast with the optical phonon.[20,22] In summary, the phonon-assisted hopping gives us the same activated T dependence with the activation energy $E_b/2$ for both the optical and acoustic phonons in the higher temperature regime, and the T dependence deviating from the activated behavior below $T_o=\hbar\omega_0/3k$ for the optical phonon and below $T_a=\hbar\omega_m/3k$ for the acoustic phonon.

Figure 2 shows that the undoped and the least-doped samples almost have the Arrhenius type of T dependence while the T dependence of the more heavily doped samples deviates appreciably from the activated behavior in the lower-temperature regime. The phonon energy evaluated roughly from the deviation temperature is much smaller than 0.15 eV (Ref. 24) of the typical optical phonon, which indicates that the hopping would be assisted by the acoustic phonon. As also suggested in Fig. 2, the temperature regime for the measurement should be regarded as higher than or comparable to T_a because of the activated T dependence in the higher regime. This permits us to apply Eq. (5) to the analysis of the experimental data even in the acoustic-phonon-assisted hopping so as to determine the values of E_b, $\hbar\omega_m$, and J. The solid curves in Fig. 2 are the theoretical ones obtained from Eq. (5), which fit to the experimental data better than those from the ISH model. Table IV summarizes the best-fitting values of E_b, $\hbar\omega_m$, and J, where the average value $\tau_{\max}$ of $\tau_{\max+}$ and $\tau_{\max-}$ was used for estimation of J. In the lightly doped hs-PA samples ($y\geq 5.0\times10^{-4}$), the value of $\hbar\omega_m$ is about 0.03 eV and almost independent of y. Since $\hbar\omega_D$ is theoretically estimated to be 0.074 eV,[24] the ratio of $\hbar\omega_D$ to $\hbar\omega_m$ gives us the value of l as 2.5, which is close to the theoretical estimation 4–5 of the charged soliton[25] rather than >10 of the polaron.[26] As a consequence, it is concluded that the charged soliton makes a main contribution to the conduction in the lightly doped hs-PA samples. This is supported by the agreement between the experimental value, approximately 0.3 eV, and the theoretical value[25] on the binding energy E_b of the charged soliton. Table IV also indicates the larger values of E_b and $\hbar\omega_m$ in the undoped and slightly doped samples, which might reflect the effect of a dopant or impurity different from I_3^-.

The phonon-assisted hopping would depend strongly on the hopping distance r between two sites since J is considered to include the factor $\exp(-r/R)$ implicitly,[23] where R is the electron decay length for the charged soliton which is estimated to be approximately 0.36 nm.[7] Because the relaxation time τ is the reciprocal of $\Gamma(0)$, dependent exponentially on r, the distribution function $\rho(r)$ of r results in the relaxation spectrum $H(\tau)$, for which the sharpness in the profile is characterized by the

TABLE IV. The best-fitting values of E_b, $\hbar\omega_m$, and J of $\tau_{\max}^{-1}$ for all the hs-PA samples by using Eq. (5).

$y\times10^{-3}$	E_b (eV)	$\hbar\omega_m$ (eV)	J (meV)
undoped	0.95	0.053	8.9
	0.69	0.046	0.98
	0.83	0.051	20
	0.61	0.044	3.9
0.5	0.39	0.032	0.069
1.3	0.39	0.035	0.19
3.0	0.30	0.030	0.59
4.1	0.31	0.033	0.48

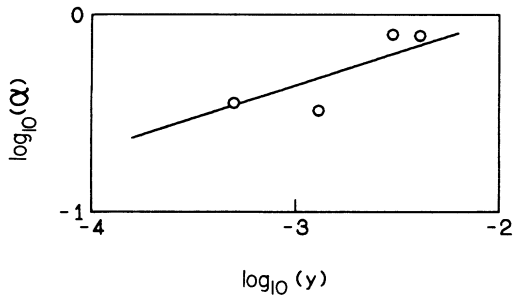

FIG. 9. Doubly logarithmic plot of α vs y for the hs-PA samples. The solid line has a slope of $\frac{1}{3}$.

exponent α in Eq. (4). By assuming that r is equal to the distance between two dopants, we will evaluate the dependence of α on the dopant concentration y in a qualitative manner.

If doping is performed homogeneously, $\rho(r)$ is given by the distribution for r in the three-dimensional random media:

$$\rho(r)=4\pi N_D r^2 \exp[-(4\pi N_D/3)r^3] . \quad (6)$$

Here N_D is the number concentration of the I_3^- dopant given by $N_D=dyN_{Av}/3M_{CH}$ where d is the density of hs-PA determined to be 1.1 g/cm^3,[11] M_{CH} the molecular weight of CH, and N_{Av} Avogadro's number. Since τ is proportional to $\exp(2r/R)$, Eq. (6) leads to the functional form of $H(\tau)$ which has the maximum value at $\ln\tau=\ln\tau_{max}$. This τ_{max} corresponds to $r_{max}=(2\pi N_D)^{-1/3}$ at which $\rho(r)$ has the maximum value. If α can be estimated roughly as $\partial \ln H(\tau)/\partial \ln\tau$ at $r=pr_{max}$ $(p<1)$, Eq. (6) gives us α as

$$\alpha=(p^{-1}-p^2)R/r_{max}$$
$$=(p^{-1}-p^2)R(2\pi dyN_{Av}/3M_{CH})^{1/3} , \quad (7)$$

which indicates that α is in proportion to $y^{1/3}$. As shown in Fig. 9, the solid line with the slope of $\frac{1}{3}$ is in a qualitative agreement with the experimental data of the lightly doped hs-PA samples ($y \geq 5.0\times10^{-4}$), and gives us the value 0.37 of p.

B. *S*-PA

The experimental results of the *S*-PA samples showed that the profile for $H(\tau)$ depends strongly on T with the parameter α proportional to T. This T dependence may be explained by the energy-dependent hopping model in which the energy difference Δ between hopping sites is taken into account. For instance, the variable range hopping[27] is one of such energy-dependent hopping models but is incompatible with the experimental results that $\mathrm{Re}(\sigma^*)$ in the frequency range over f_r depends strongly on T and has the slope s of f^s much smaller than 0.8. The phonon-assisted hopping between nonequivalent sites as an energy-dependent hopping model, on the other hand, was dealt with in the same formalism as the hopping between equivalent sites,[21] which indicated that, except for the extremely large Δ and low temperature, the hopping rate for jumps between nonequivalent sites is evaluated simply from the rate for jumps between equivalent sites as $\Gamma(\Delta)=\exp(-\Delta/2kT)\Gamma(0)$.[28] Thus, if the distribution $\rho(\Delta)$ of Δ is broad enough in comparison with $\rho(r)$, $H(\tau)$ mainly arises from $\rho(\Delta)$, so that the profile for $H(\tau)$ would have a strong T dependence.[29] In contrast, the experimental results of hs-PA showed that the conduction mechanism of hs-PA was ascribed to the isoenergetic hopping as mentioned earlier, which means the dominant contribution of $\rho(r)$ to $H(\tau)$. These results suggest the considerable difference between hs-PA and *S*-PA in the dispersion of $\rho(\Delta)$. However, other experimental results which compared hs-PA with *S*-PA by x-ray diffractometry,[30] ir, and resonance Raman spectroscopy[10] indicated that there was no distinct difference between them in crystal structure and conformation. Thus, it is not easy to accept that *S*-PA alone has a largely dispersive $\rho(\Delta)$, although it can explain the T-dependent profile for $H(\tau)$. We should consider another energy-dependent hopping model as a conduction mechanism of *S*-PA.

Barrier hopping[31,32] is also regarded as an energy-dependent hopping model, since the height W of the potential barrier between two hopping sites has a broad distribution $\rho(W)$ in general which leads to a large dispersion in the activation energy. Here we will consider that a carrier (charged soliton) bound to a dopant by the Coulombic attractive force hops to a site close to another dopant located on a different chain, since the interchain hopping would make a main contribution to the conductivity in a low-frequency region. Then W is defined by[31]

$$W_0-W=e^2/\pi\epsilon_0\epsilon_s r , \quad (8)$$

where W_0 is the energy difference between the ground and the extended states,[31,32] e the elementary charge, and ϵ_s the dielectric constant. Equation (8) indicates that since W increases with ϵ_s, the small ϵ_s facilitates the long-range hopping of the carrier owing to the low potential barrier. Incidentally, ϵ_s of PA was estimated from our experimental results of hs-PA to be approximately 7. As mentioned in Sec. I, *S*-PA has the fibrillar structure in which fibrils are entangled and a lot of empty spaces are observed.[2] Since ϵ_s is nearly the unity in the interfibril hopping between surfaces of two fibrils, the barrier hopping would be more favorable for the interfibril jump than for the intrafibril one. Thus, it is possible that the interfibril barrier hopping makes a main contribution to the conduction mechanism in *S*-PA. (Within the fibril of *S*-PA, the intermolecular phonon-assisted hopping may dominate as well as in hs-PA.)

As suggested in Eq. (8), the distribution function $\rho(r)$ of r in the barrier hopping yields $\rho(W)$, which leads to $H(\tau)$ through the relation $\tau\propto\exp(W/kT)$. Then $\alpha=\partial \ln H(\tau)\partial \ln\tau$ is written

$$\alpha=\partial \ln H(\tau)/\partial \ln\tau=kT\partial \ln\rho(W)/\partial W ,$$

which is rewritten by using Eq. (8) as

$$\alpha=(\pi kT\epsilon_0\epsilon_s/e^2)[r^2\partial \ln\rho(r)/\partial r+2r] . \quad (9)$$

TABLE V. The values of r_0 and S which are estimated from W_{max} and kT/α by using Eqs. (12) and (13) in all the S-PA samples.

$y\times10^{-3}$	$\sigma(0)$ (Sm^{-1}) at RT	W_{max} (eV)	kT/α (eV)	r_0 (nm)	S (nm)
undoped	5.79×10^{-5}	0.36	0.024	17	1.9
0.48	2.06×10^{-3}	0.29	0.022	14	1.3
1.3	5.51×10^{-3}	0.20	0.019	11	0.92
3.9	1.24×10^{-2}	0.14	0.017	10	0.73

Equation (9) indicates that α is proportional to T, which agrees with the experimental results of S-PA as shown in Fig. 7. In addition, the proportional constant gives us $\partial \ln\rho(r)/\partial \ln r$, which represents the sharpness in the profile for $\rho(r)$. If $\rho(r)$ is assumed to be a Gaussian distribution,

$$\rho(r)=[(2\pi)^{-1/2}/S]\exp[-(r-r_0)^2/2S^2] , \quad (10)$$

with the peak at r_0 and the width S, the substitution of Eq. (10) into Eq. (9) yields

$$\partial \ln H(\tau)/\partial \ln\tau = kT(\pi\epsilon_0\epsilon_s/e^2)[(r_0-r)r^2/S^2+2r] . \quad (11)$$

Equation (11) indicates that $H(\tau)$ has the functional form similar to that for the positive α in Eq. (4), i.e., the asymmetric profile characterized by the steep decrease at $r>r_{max}$ and the long tail at $r<r_{max}$, where r_{max} is derived from $\partial \ln H(\tau)/\partial \ln\tau=0$ as

$$(r_0-r_{max})r_{max}^2/S^2+2r_{max}=0 . \quad (12)$$

Then, α could be estimated roughly as the maximum value of $\partial \ln H(\tau)/\partial \ln\tau$ in $0<r<r_{max}$ by

$$\alpha=kT(\pi\epsilon_0\epsilon_s/e^2)[(r_0-r_1)r_1^2/S^2+2r_1] , \quad (13)$$

where r_1 is given by $2r_0r_1-3r_1^2+2S^2=0$.

The experimental results of S-PA can give us the proportional constant α/T from Fig. 7 and the activation energy W_{max} of τ_{max}^{-1} from Fig. 8, which is related to r_{max} by Eq. (8). (A small deviation from the Arrhenius type in τ_{max}^{-1} might be due to the influence of the tunneling conduction.[33]) Thus, we obtained r_0 and S from W_{max} and α/T by using Eqs. (12) and (13) as summarized in Table V. Since the diameter of the fibrils in S-PA was estimated to be approximately 20 nm,[2] the values of r_0 obtained are reasonable ones. As a consequence, both the experimental results of α proportional to T and the hopping distance of almost the same length as the fibril diameter lead us to the conclusion that the interfibril barrier hopping contributes mainly to the conduction mechanism of S-PA.

This conclusion is also supported by the experimental results of the different non-Ohmic behavior between hs-PA and S-PA. The phonon-assisted hopping theory predicts a large non-Ohmic behavior which manifests itself in the applied voltage V between two hopping sites greater than $V_n=2kT/e$.[21] Thus, the nonlinearity increases gradually with decreasing T owing to the reduction of V_n, which agrees with the experimental result of the T dependence of the non-Ohmic behavior in hs-PA as mentioned in Sec. III. Thus, the experimental results of the non-Ohmic behavior support the conclusion that the conduction mechanism of hs-PA is ascribed to the phonon-assisted hopping.

In the barrier hopping, on the other hand, V_n should be estimated as the applied voltage that exerts significant influence on the barrier height W. When the electric field V/r is applied to two sites located at $x=0$ and $x=r$ in the direction parallel to the x axis, the electric potential energy $W(x,V)$ between two sites is given by

$$W(x,V)=W_0-e^2r/4\pi\epsilon_0\epsilon_s x(r-x)-(eV/r)x . \quad (14)$$

The maximum value of $W(x,V)$ with respect to x affords the V-dependent height $W(V)$ of the potential barrier. For simplicity, we employ the parabolic-barrier approximation[33] in which the Coulombic potential in Eq. (14) is replaced with the parabolic potential as

$$W(x,V)=[4W(0)/r^2]x(r-x)-(eV/r)x , \quad (15)$$

where $W(0)$, given by $W(0)=W_0-e^2/\pi\epsilon_0\epsilon_s r$, denotes the barrier height in the absence of the applied electric field. Since Eq. (15) gives us the maximum value of $W(x,V)$ as

$$W(V)=[4W(0)-eV]^2/16W(0) , \quad (16)$$

the effect of the external voltage between two sites on the barrier height manifests itself in $V>V_n\sim4W(0)/e$. Since the largest voltage should be applied to the highest potential barrier W_{max}, we can estimate $W(0)$ to be approximately 0.3 eV of W_{max} much greater than kT from Table V. Thus, it is concluded that the nonlinearity of the barrier hopping is much smaller than that of the phonon-assisted hopping. The experimental results of the negligibly small non-Ohmic behavior in S-PA compared with hs-PA supports the conclusion that the barrier hopping contributes mainly to the conduction mechanism of S-PA.

V. CONCLUSION

The f and T dependence of σ^* was measured for the undoped and lightly doped films of hs-PA and S-PA. The data analysis based on the conductivity relaxation formalism leads us to the findings that the functional form of $H(\tau)\propto\tau^\alpha$ ($\tau_{min}<\tau<\tau_{max}$, $-1<\alpha<1$) fitted the experimental data best and that α of hs-PA was independent of T while α of S-PA was proportional to T. The T-independent α of hs-PA indicates the isoenergetic hop-

ping between equivalent sites, so that the conduction mechanism of hs-PA can be ascribed to the acoustic phonon-assisted hopping of the charged soliton between PA chains. On the other hand, it is likely that the interfibril barrier hopping makes a main contribution to the conduction mechanism of *S*-PA since the small ϵ_s in the interfibril hopping facilitates the barrier hopping between fibrils. Thus, the different conduction mechanism between hs-PA and *S*-PA should arise from their morphological dissimilarities. This conclusion was supported by the experimental result that hs-PA showed a non-Ohmic behavior much greater than *S*-PA.

Comparing Fig. 2 with Fig. 5, one may notice little difference between hs-PA and *S*-PA in the T dependence of $\sigma(0)$. As mentioned so far, the different conduction mechanism between them was revealed by the σ^* measurement leading to $H(\tau)$ through the data analysis based on the conductivity relaxation formalism. In general, it would be difficult to determine the conduction mechanism from the experimental data of $\sigma(0)$ alone in undoped and lightly doped conducting polymers, since both the T dependence of a hopping rate and the profile for $H(\tau)$ affect that of $\sigma(0)$ at the same time. Then, the σ^* measurement enables us to distinguish the T dependence of a hopping rate and to discuss the conduction mechanism in the light of the distribution of the hopping rates.

---

*To whom all correspondence should be addressed.

†Present address: Department of Applied Physics, Faculty of Engineering, University of Tokyo, Bunkyo-ku, Tokyo 113, Japan.

[1] *Handbook of Conducting Polymers,* edited by T. A. Skotheim (Mercel Dekker, New York, 1986).

[2] J. C. W. Chien, *Polyacetylene* (Academic, New York, 1984).

[3] J. R. MacDonald, *Impedance Spectroscopy* (Wiley, New York, 1987).

[4] S. Roth and H. Bleier, Adv. Phys. **36**, 385 (1987).

[5] A. J. Epstein, H. Rommelmann, M. Abkowitz, and H. W. Gibson, Mol. Cryst. Liq. Cryst. **77**, 81 (1981).

[6] T. Ito, H. Shirakawa, and S. Ikeda, J. Polym. Sci. Polym. Chem. Ed. **12**, 11 (1974).

[7] S. Kivelson, Phys. Rev. B **25**, 3798 (1982).

[8] J. A. Chroboczek and S. Summerfield, J. Phys. (Paris) Colloq. **44**, C3-517 (1983).

[9] H. Naarman and N. Theophilou, Synth. Met. **22**, 1 (1987).

[10] J. Tsukamoto, A. Takahashi, and K. Kawasaki, Jpn. J. Appl. Phys. **29**, 125 (1990).

[11] K. Akagi, M. Suezaki, H. Shirakawa, H. Kyotani, M. Shimomura, and Y. Tanabe, Synth. Met. **28**, D1 (1989).

[12] H. Kyotani, M. Shimomura, Y. Tanabe, Y. Watanabe, M. Suezaki, T. Kasai, K. Akagi, and H. Shirakawa, Rep. Prog. Polym. Phys. Jpn. **31**, 265 (1988).

[13] R. Hayakawa and Y. Wada, IEE Conf. Pub. **177**, 396 (1979).

[14] K. Ito, Y. Tanabe, K. Akagi, M. Suezaki, T. Kasai, and H. Shirakawa, Rep. Prog. Polym. Phys. Jpn. **32**, 337 (1989).

[15] K. L. Ngai and R. W. Rendell, in *Handbook of Conducting Polymers,* edited by T. A. Skotheim (Mercel Dekker, New York, 1986), pp. 967–1039.

[16] M. Lax and T. Odagaki, in *Random Walks and their Applications in the Physical and Biological Sciences* (National Bureau of Standards, Washington, D.C.), Proceedings of a Conference on Random Walks and their Applications in the Physical and Biological Sciences, edited by Michael F. Shlesinger and Bruce J. West, AIP Conf. Proc. No. 109 (AIP, New York, 1982), p. 133.

[17] H. Scher and M. Lax, Phys. Rev. B **7**, 4491 (1973); **7**, 4502 (1973).

[18] T. Odagaki and M. Lax, Phys. Rev. B **24**, 5284 (1981).

[19] S. Kivelson and A. J. Epstein, Phys. Rev. B **29**, 3336 (1984).

[20] D. Emin, Phys. Rev. Lett. **32**, 303 (1974).

[21] D. Emin, Adv. Phys. **24**, 305 (1975).

[22] E. Gorham-Bergeron and D. Emin, Phys. Rev. B **15**, 3667 (1977).

[23] K. Shimakawa and K. Miyake, Phys. Rev. B **39**, 7578 (1989); K. Shimakawa, *ibid.* **39**, 12 933 (1989).

[24] E. J. Mele and M. J. Rice, Solid State Commun. **34**, 339 (1980).

[25] W. P. Su, J. R. Schrieffer, and A. J. Heeger, Phys. Rev. B **22**, 2099 (1980).

[26] D. K. Campbell and A. R. Bishop, Phys. Rev. B **24**, 4859 (1981).

[27] N. F. Mott and E. A. Davis, *Electronic Process in Non-Crystalline Materials* (Clarendon, Oxford, 1979).

[28] D. Emin, in *Handbook of Conducting Polymers,* edited by T. A. Skotheim (Mercel Dekker, New York, 1986), pp. 915–936.

[29] K. Ito and Y. Tanabe, Rep. Prog. Polym. Phys. Jpn. **33**, 381 (1990).

[30] H. Kyotani, M. Shimomura, Y. Tanabe, K. Akagi, T. Kasai, Y. Zhang, and H. Shirakawa, Rep. Prog. Polym. Phys. Jpn. **33**, 205 (1990).

[31] G. E. Pike, Phys. Rev. B **6**, 1572 (1972).

[32] S. R. Elliott, Philos. Mag. **36**, 1291 (1977); **37**, 553 (1978).

[33] P. Sheng, Phys. Rev. B **21**, 2180 (1980).